AFRL-SR-AR-TR-09-0175

REPORT DOCUMENTATION PAGE

PLEASE DO NOT RETURN YOUR FORM TO THE ABOVE ORGANIZATION.

1. REPORT DATE *(DD-MM-YYYY)*	2. REPORT TYPE	3. DATES COVERED *(From - To)*
19-05-2009		from 2005 to 2008

4. TITLE AND SUBTITLE
Flow Simulations:
The Lagrangian Averaged Navier-stokes Equations and optimization

5a. CONTRACT NUMBER
FA9550-05-1-0334

5b. GRANT NUMBER

5c. PROGRAM ELEMENT NUMBER

6. AUTHOR(S)
Kamran Mohseni

5d. PROJECT NUMBER
1541913

5e. TASK NUMBER

5f. WORK UNIT NUMBER

7. PERFORMING ORGANIZATION NAME(S) AND ADDRESS(ES)
Department of Aerospace Engineering Sciences
University of Colorado
Boulder, CO 80309-429

8. PERFORMING ORGANIZATION REPORT NUMBER

9. SPONSORING/MONITORING AGENCY NAME(S) AND ADDRESS(ES)
AFOSR
875 N RANDOLPH ST
ARLINGTON, VA 22203
DR. FARIBA FAHROO

10. SPONSOR/MONITOR'S ACRONYM(S)

11. SPONSOR/MONITOR'S REPORT NUMBER(S)

12. DISTRIBUTION/AVAILABILITY STATEMENT

DISTRIBUTION A: APPROVED FOR PUBLIC RELEASE

13. SUPPLEMENTARY NOTES

14. ABSTRACT

This project had two objectives in using Lagrangian techniques and their application in flows. The first research thrust area was to develop a modeling technique that will allow for efficient computation of compressible flows which could include simulations involving both shock and turbulent behavior. Spatial averaging of the nonlinear convective term was applied to the Burgers and Euler equations.

The second research thrust area was the development of Lagrangian averaging tools for analyzing flow over a lifting airfoil. Stable and unstable manifolds were computed and finite time Lyapanov exponent (FTLE) of the flow map was used to identify Lagrangian coherent structures in complex unsteady flow around an Eppler 387 airfoil. The unstable and stable manifolds identify the separation and reattachment points respectively.

15. SUBJECT TERMS
shock regularization, vortex shedding

16. SECURITY CLASSIFICATION OF:			17. LIMITATION OF ABSTRACT	18. NUMBER OF PAGES	19a. NAME OF RESPONSIBLE PERSON
a. REPORT	b. ABSTRACT	c. THIS PAGE			19b. TELEPHONE NUMBER *(Include area code)*

Flow Simulations:
The Lagrangian Averaged Navier-stokes Equations and optimization

FA9550-05-1-0334

Kamran Mohseni
Department of Aerospace Engineering
University of Colorado, Boulder

Abstract

This project had two objectives in using Lagrangian techniques and their application in flows. The pinnacle goal of first research thrust area was to develop a modeling technique that will allow for efficient computation of compressible flows which could include simulations involving both shock and turbulent behavior. Spatial averaging of the nonlinear convective term was applied initially to the Burgers equation, which is a very simplistic model for compressible shocks and turbulence. During the course of the research the solutions to the modified Burgers equation have been proven to exist and converge to the physically relevant solution as the spatial averaging is reduced. Numerical simulations were conducted on the modified equations showing proper wave propagation and energy decay results. This technique was then extend into the Euler equations with promising preliminary results.

The second research thrust area was the development of Lagrangian averaging tools for analyzing flow over a lifting airfoil. Lagrangian techniques have been recently used in defining coherent structures (LCS) in flows. In this case, stable and unstable manifolds were computed. Intersection of these manifolds define lobes with distinct mixing behavior. Finite time Lyapanov exponent (FTLE) of the flow map was used to identify Lagrangian coherent structures in complex unsteady flow around an Eppler 387 airfoil. The unstable and stable manifolds identify the separation and reattachment points respectively.

1 Shock Regularization

Introduction No one can deny the importance of fluid dynamics in the modern world. It can be seen everyday in planes flying through the sky to the running water in our sinks. The governing equations of fluid dynamics, the Euler and Navier-Stokes equations have been well known for over 200 year, but still much is unknown. The nonlinear structure found in both the equations present serious difficulties. Shocks and turbulence are the two main fluid behaviors that are computationally difficult. Both of these phenomenon develop as a result of the nonlinear terms and the small scales that they produce. If one were to properly model the effect of these small scales then it is possible to produce a technique that could simultaneously capture both turbulence and shocks. It is towards this goal that the research presented here has been developed.

One of the methods that has recently met with quite a bit of success in modeling certain turbulent flows is the Lagrangian Averaging method [1; 2; 3; 4; 5; 6; 7; 8; 9; 10]. This method was applied to incompressible flow resulting in the Lagrangian Averaged Navier Stokes (LANS-α) equations where a filtered convective velocity was introduced in the nonlinear term. It was this work that provided the inspiration and beginnings of the research presented here.

The goal this research is to devclop a similar method of modeling compressible flows. It was intuited that it was the modified nonlinear term $\bar{\mathbf{u}} \cdot \nabla \mathbf{u}$ that was the key to the LANS-α equation and that a similar term could be introduced into the equations for compressible flow. To examine the effect of this nonlinear term in compressible flow it was inserted into an extremely simplified model of compressible flow, the inviscid Burgers equation resulting in the equations

$$\mathbf{u}_t + \bar{\mathbf{u}} \cdot \nabla \mathbf{u} = 0 \tag{1a}$$

$$\bar{\mathbf{u}} = g^\alpha * \mathbf{u} \tag{1b}$$

$$g^\alpha = \frac{1}{\alpha} g(\frac{\mathbf{x}}{\alpha}). \tag{1c}$$

where g represents the spatial filter and α represents the amount of filtering. These equations are referred to as the Convectively Filtered Burgers (CFB) equations. The following section summarizes the research that has been accomplished regarding these equations.

1.1 Burgers Equation

It is of upmost importance that the CFB equations capture the behavior of the original equations while remaining regularized. In order to demonstrate this the research has proven that the CFB equations will converge to the solutions of the inviscid Burgers equations,

$$\mathbf{u}_t + \mathbf{u} \cdot \nabla \mathbf{u} = 0, \tag{2}$$

as the spatial filtering is reduced. This was accomplish in three steps

- Prove that the solutions to the CFB equations exist and are unique
- Prove that as the filtering is reduced, as $\alpha \to 0$, the solutions of the CFB equations converge to weak solutions of the inviscid Burgers equation.
- Prove that those weak solutions are the physically relevant solution, i.e. the entropy solution.

In the course of the research the following theorems were proven addressing these steps. The first theorem establishes that solutions to the modified Burgers equations exist and are unique. It also establishes the fact that the solutions are in fact continuous and will remain so throughout time.

Theorem 1.1 *Let $g(\mathbf{x}) \in W^{1,1}(\mathbb{R}^n)$ and $\mathbf{u}_0(\mathbf{x}) \in C^1(\mathbb{R}^n)$, then there exists a unique global solution $\mathbf{u}(\mathbf{x}, t) \in C^1(\mathbb{R}^n, \mathbb{R})$ to the initial value problem (3).*

$$\mathbf{u}_t + \bar{\mathbf{u}} \cdot \nabla \mathbf{u} = 0 \tag{3a}$$

$$\bar{\mathbf{u}} = g * \mathbf{u} \tag{3b}$$

$$\mathbf{u}(\mathbf{x}, 0) = \mathbf{u}_0(\mathbf{x}) \tag{3c}$$

The next theorem establishes that as the spatial filtering decreases the solutions will converge to a weak solution of the inviscid Burgers equations. This additionally establishes that the shock speeds found in the CFB equations will be the same as those of the original equations.

Theorem 1.2 *For any g which Fourier transform is of the form*

$$\hat{g}(k) = \frac{1}{1 + \sum_{j=1}^{n} C_j k^{2j}} \qquad \text{with } n < \infty, C_j \geq 0 \; C_n \neq 0,$$

the solutions to the CFB equations converge to a weak solution of the inviscid Burgers equation.

Finally the next theorem establishes that for specific initial conditions the solutions will converge to the entropy solution of inviscid Burgers equations.

Theorem 1.3 *The solutions of the CFB equations converge to the entropy solution of the inviscid Burgers equation for continuous bell-shaped initial conditions.*

A conjecture was then put forward and while not proven was supported with substantial reasoning.

Conjecture 1.4 *The solutions u^α of the CFB equations converge to the entropy solution of the inviscid Burgers equation for continuous initial conditions as $\alpha \to 0$.*

If this conjecture is assumed to be true then the equations paired with a filtered initial condition

$$u_t + (u * g^\alpha) u_x = 0 \tag{4a}$$

$$u(x, 0) = u_0 * g^\alpha \tag{4b}$$

will converge to the entropy solution for any bounded initial condition.

Thus through analytical means it was proven that this use of spatial averaging in the nonlinear term will successfully regularize Burgers equation and will capture the physical behavior of the original equation.

Numerical Results In order to more thoroughly understand the CFB equations, numerical simulations were run. In figure 1 the behavior of a pulse under the CFB equations can be seen. The pulse will steepen and from a shock front as time progresses, but remain continuous.

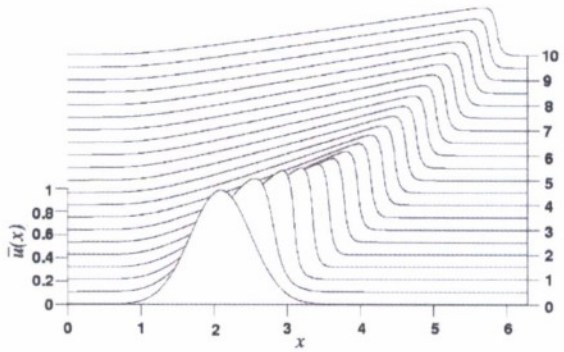

Figure 1: Evolution of the CFB equations. Here a smooth pulse can be seen evolving into a shock front, but remaining continuous.

Figure 2 compares the solutions of the CFB equations to the solutions of the inviscid Burgers equation. It demonstrates the CFB equations capture both the shock and expansion wave behavior found in Burgers equation.

In addition to general behavior of the CFB equations it was shown with numerical techniques that the thickness of the shocks can be controlled by varying the parameter α. Additionally α controls energy decay which was found to be similar to that of the viscous Burgers equation. The spectral energy profile was also examined where it was seen that the choice of the spatial filter, g, greatly affects the spectral energy decomposition and controls the degree of smoothness of the solutions.

This research has led to several journal publications [11; 12] and conference papers [13; 14; 7]. It also made up a significant portion of a graduate student's thesis [15].

1.2 Euler equations

While the successful regularization of the Burgers equation is a good starting point, in order to have real world applications research into the Euler equations has begun. Recently preliminary examinations into a regularization of the Euler equations have begun with promising initial results. Both the Euler and homentropic Euler equations have been examined. In both cases the nonlinear terms of the equations have been modified in a similar manner as the Burgers equation. For the homentropic Euler equations the modified equations are

$$\rho_t + \bar{\rho} u_x + \bar{u} \rho_x = 0 \tag{5a}$$

$$(\rho u)_t + (\overline{\rho u}) u_x + \bar{u} (\rho u)_x + P_x = 0. \tag{5b}$$

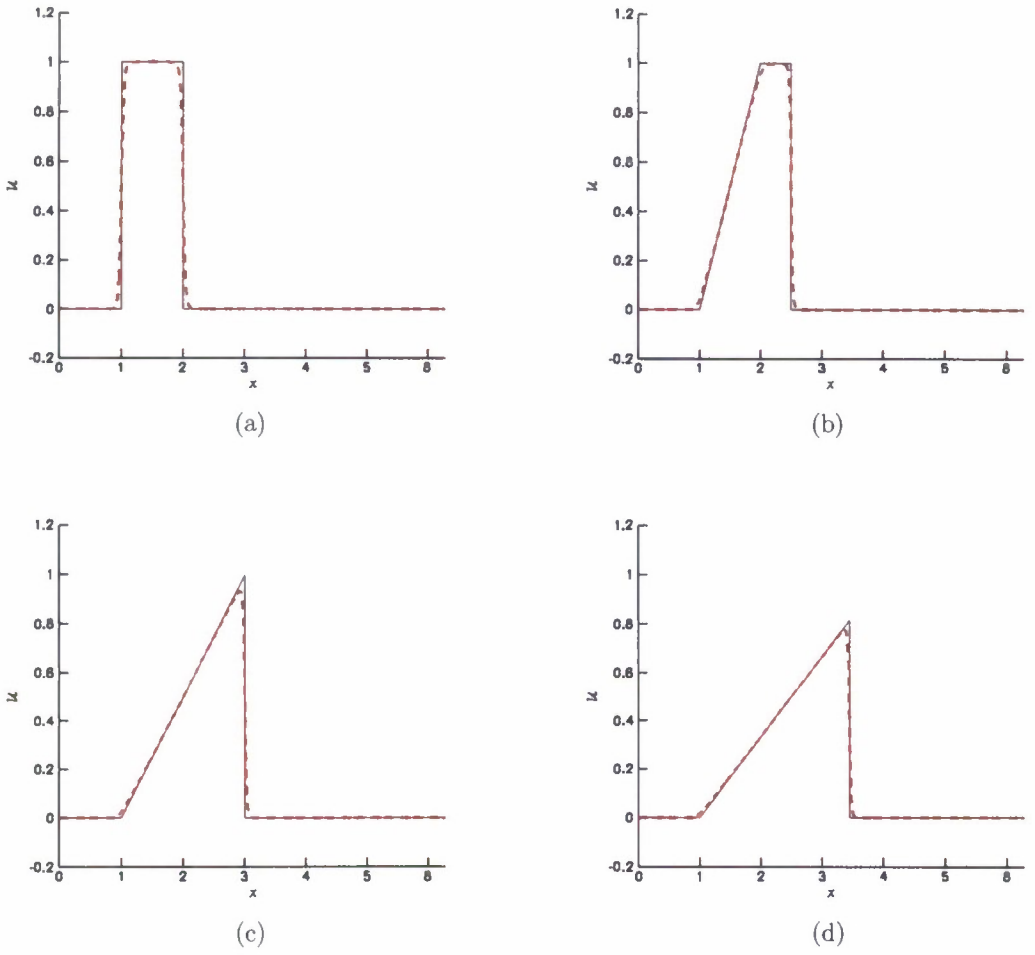

Figure 2: This figure compares the entropy solution of inviscid Burgers equation with the solution to the CFB equations for $\alpha = 0.02$. It is easy to see that the CFB solution is capturing both the rarefaction wave and the shock front behavior.

where the bar represents the spatial filtering as before and the pressure, P, is purely a function of the density.. The equations for the Euler equations without the homentropic assumption are

$$\rho_t + \bar{\rho} u_x + \bar{u} \rho_x = 0 \tag{6a}$$

$$(\rho u)_t + \overline{\rho u} u_x + \bar{u} (\rho u)_x + P_x = 0 \tag{6b}$$

$$(\rho e)_t + \overline{\rho e} u_x + \bar{u} (\rho e)_x + \overline{P} u_x + \bar{u} P_x = 0 \tag{6c}$$

$$P = (\gamma - 1) \left(\rho e - \frac{1}{2} \rho u^2 \right). \tag{6d}$$

With analytical techniques these equations have been proven to converge to weak solutions of the original equation provided modest assumptions on the solutions. Numerically the equations are shown promising behavior. The solution appear to be well regularized and capture much of the behavior of the original equations. Figure 3 shows a double shock tube simulation for the modified homentropic Euler equations

plotted against the solution to the original homentropic Euler equations. Both the expansion wave and shock behavior are being captured. Figure 4 shows a shock tube simulation for the Euler equations. The modified equations are showing a regularized solution that is capturing the expansion wave, contact surface, and shock.

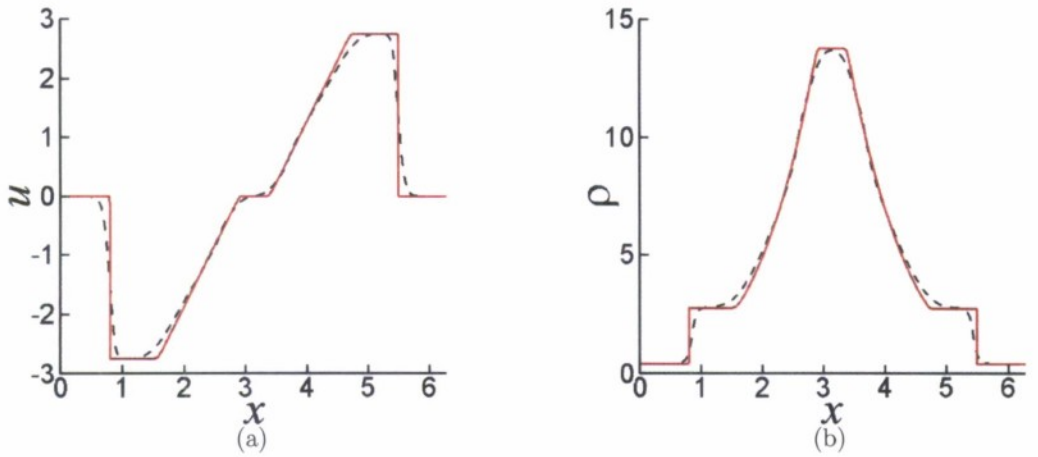

Figure 3: This figure shows a numerical simulation of the modified homentropic Euler equations (dashed line) plotted against the solution to the homentropic Euler equations (solid line). Here the value of $\alpha = 0.05$. In both figures it is clear that the modified homentropic Euler equations are capturing both the expansion wave and shock behavior. (a) The velocity. (b) The density.

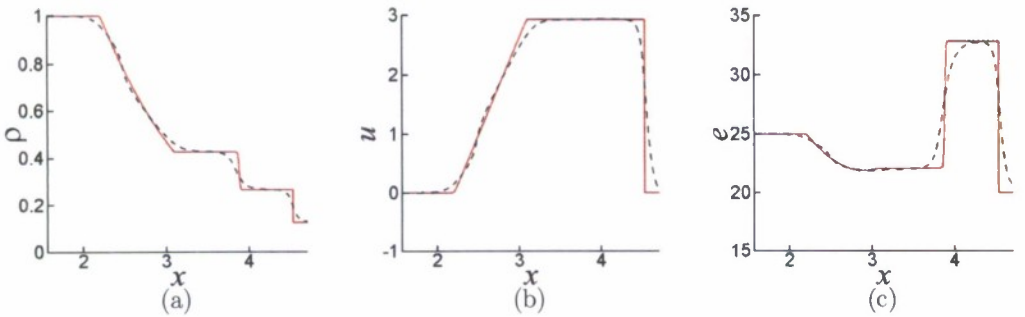

Figure 4: This figure shows a numerical simulation of the modified Euler equations (dashed line) plotted against the solution to the Euler equations (solid line). Here the value of $\alpha = 0.05$. In the figures it is clear that the modified Euler equations are capturing both the expansion wave, contact surface, and shock behavior. (a) The density. (b) The velocity. (c) The energy.

Future work in this area includes proving the existence and uniqueness of the results for 1D and higher dimensional Euler equation, extensive numerical simulation to characterize the equations in 1D and multi-dimensions, and performing a shock turbulence simulations in 3D.

2 Computation of Coherent Structures at Low Re

In this section we will use Lagrangian techniques in order to understand the unsteady vortex shedding around an airfoil. In particular we use a new Lagrangian approach; namely Lagrangian Coherent Structures (LCS) [16; 17]. Lagrangian Coherent Structures are invarient material manifolds that can be identified through carefull study of particle mixing behavior. These manifolds are responsible for the organization of mixing in the wake of an airfoil, and hold the potential for new insights into the understanding of active flow control. Lagrangian Coherent Structures can be an important tool in achieving this goal. As we will demonstate, LCS can be very usefull in identifying the separation manifolds, and the energetics of flow structures within the separation bubble.

In persuit of this goal, our group has developed software that allows for detailed computation of LCS manifolds in two-dimensional Naiver-Stokes flow. The software has been used to expose manifolds in the separated region which were previously hidden by traditional flow maps and Eulerian approach.

Figure 5: Where the particles come from in a shed vortex behind a 2D airfoil? Stable and unstable manifold identify the boundaries of regions with different mixing behavior. Colors represent drifters in the flow. Different colors are separated by the stable and unstable manifolds. The region confined between a stable and unstable manifold form a lobe which has a distinct mixing property. See Cardwell and Mohseni [20].

Lagrangian coherent structures (LCS). Lagrangian coherent structures provide a method of analyzing a flow field from a dynamical systems perspective. LCS were introduced by [18] and further defined by [17]. LCS represent lines of negligible fluid flux in a flow and therefore govern transport and mixing in the flow.

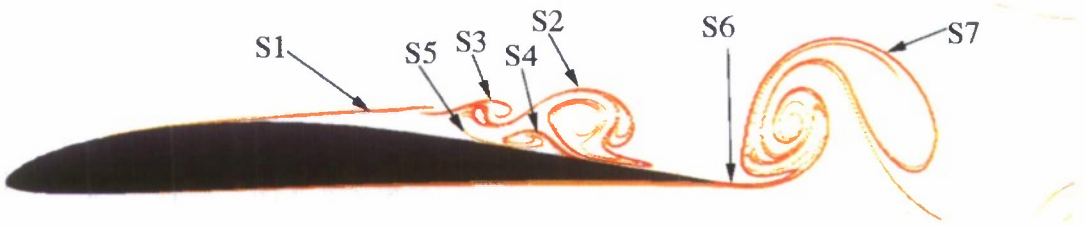

Figure 6: Contour plots of FTLE over airfoil at time = 0.00, S1-S7 are the major recurring structures in the flow

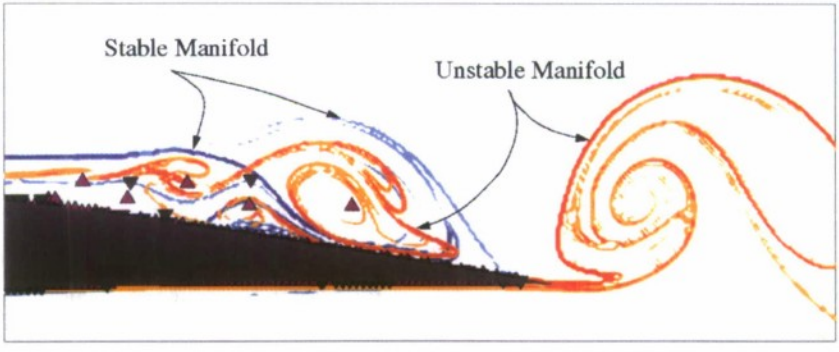

Figure 7: Stable and Unstable manifolds overlayed showing potential for lobe analysis. The figure also shows locations of several stagnation points in the flow, ▲ designate elliptic stagnation points, ▼ designate hyperbolic stagnation points. Unstable manifolds characterize the separation lines while stable manifolds can be used to identify the reattachment lines.

Due to the general framework provided by LCS, they have been applied to a wide range of different areas including pollution transport in the ocean [19], two-dimensional turbulence [18; 20], vortex shedding behind an airfoil in our group [21; 22], and transport in empirical vortex rings and hydromedusa swimming [23; 24]. They have proven to be an effective tool for identifying exact vortex boundaries and can be used to divide a flow into lobes which govern the transport [25]. We follow the procedure for computing LCS outlined by [17] and we provide here a brief overview for those unfamiliar with this concept.

We use CFd results around an Eppler 387 in order to calculate the finite time Lyapunov Exponent (FTLE). The resulting FTLE field depends on the integration time, T, in that larger values of T reveal more structures than smaller values of T so T may be chosen to reveal the desired level of detail without worrying about influencing the major structures which are revealed. Additionally, T may be positive or negative, representing forward and backward particle advection respectively. Therefore, there are two types of FTLE fields, forward time and backward time.

Once the FTLE eld has been calculated, LCS are dened as ridges in the FTLE eld [17]. In practice, LCS are usually visualized by looking at contour plots of the FTLE eld. Conceptually, ridges in the forward FTLE field, called forward LCS, represent lines where particles diverge most quickly and backward LCS represent lines where particles converge. For this region, dye visualization experiments reveal structures very similar to backward LCS. Additionally, for LCS which are sufciently strong, the flux across the LCS is negligible, a property which makes LCS extremely useful for analyzing transport in flows. Finally, forward LCS are analogous to the stable manifolds of a dynamical system and act as repelling material lines while backward LCS are analogous to the unstable manifolds of a dynamical system and act as attracting material lines. The interaction of these LCS largely govern transport in a flow and their intersections can be used to exactly dene a vortex without the use of arbitrary thresholds of vorticity [23].

Example of LCS Calculation for Flow Over an Airfoil and Flow Structure Interaction Problems. We have developed LCS computational capabilities for flow around fixed and deforming objects in unstructured mesh; see Cardwell & Mohseni [26; 22]. We have primarily analyzed low Reynolds number (Re) flows over airfoils [27; 28; 29; 27; 26; 22]. One of the largest efforts was a study on where the fluid in vortices shed behind an airfoil originates [27; 28]. Further references on LCS are available at [17; 30; 19; 31; 27; 32; 23; 33]. LCS allow the application of well understood dynamical systems techniques to analysis of 2D aperiodic flows which may come from experimental or CFD data.

References

[1] A. Cheskidov, D.D. Holm, E. Olson, and E.S. Titi. On a Leray-α model of turbulence. *Royal Society London, Proceedings, Series A, Mathematical, Physical & Engineering Sciences*, 461(2055):629–649, 2004.

[2] C. Foias, D. D. Holm, and E. S. Titi. The Navier-Stoke-α model of fluid turbulence. *Physica D.*, 152-3:505–519, 2001.

[3] C. Foias, D.D. Holm, and E.S. Titi. The three dimensional viscous Camassa-Holm equations, and their relation to the Navier-Stokes equations and turbulence theory. *Journal of Dynamics and Differential Equations.*, 14(1):1–35, 2002.

[4] J.E. Marsden and S. Shkoller. Global well-posedness of the LANS-α equations. *Proc. Roy. Soc. London*, 359:1449–1468, 2001.

[5] K. Mohseni, B. Kosović, S. Shkoller, and J.E. Marsden. Numerical simulations of the Lagrangian averaged Navier-Stokes (LANS-α) equations for homogeneous isotropic turbulence. *Phys. Fluids*, 15(2):524–544, 2003.

[6] H. Zhao and K. Mohseni. A dynamic model for the Lagrangian averaged Navier-Stokes-α equations. *Phys. Fluids*, 17(7):075106, 2005.

[7] K. Mohseni, H. Zhao, and J. Marsden. Shock regularization for the burgers equation. AIAA paper 2006-1516, 44$^{\text{th}}$ AIAA Aerospace Sciences Meeting and Exhibit, Reno, Nevada, January 9-12 2006.

[8] H. S. Bhat, R. C. Fetecau, J. E. Marsden, K. Mohseni, and M. West. Lagrangian averaging for compressible fluids. *SIAM Journal on Multiscale Modeling and Simulation*, 3(4):818–837, 2005.

[9] D.D. Holm, J.E. Marsden, and T.S. Ratiu. Euler-Poincaré models of ideal fluids with nonlinear dispersion. *Phys. Rev. Lett.*, 349:4173–4177, 1998.

[10] S.Y. Chen, D.D. Holm, L.G. Margoin, and R. Zhang. Direct numerical simulations of the Navier-Stokes-*alpha* model. *Physica D*, 133:66–83, 1999.

[11] G. Norgard and K. Mohseni. A regularization of the Burgers equation using a filtered convective velocity. *J. Phys. A: Math. Theor.*, 41:1–21, 2008.

[12] G. Norgard and K. Mohseni. Convergence of convectively filtered Burgers equation to the entropy solution of inviscid Burgers equation. Accepted to siam journal, multiscale modeling and simulation., 2009. Also http://arxiv.org/abs/0805.2176.

[13] G. Norgard and K. Mohseni. A regularization of Burgers equation using a filtered convective velocity. AIAA paper 2007-0714, 45$^{\text{th}}$ AIAA Aerospace Sciences Meeting and Exhibit, Reno, Nevada, January 8-11 2007.

[14] G. Norgard and K. Mohseni. Convectively filtered Burgers in one and multiple dimensions. AIAA paper 2007-4221, 37$^{\text{th}}$ AIAA Fluid Dynamics Conference and Exhibit, Miami, FL, June 25 - 28 2007.

[15] G.J. Norgard. *Shock Regularization of Conservation Laws Through Use of Spatial Averaging in Nonlinear Terms.* PhD thesis, University of Colorado Boulder, CO, May 2009.

[16] G. Haller. Distinguished material surfaces and coherent structures in three-dimensional fluid flows. *Physica D*, 149:248–277, 2001.

[17] S.C. Shadden, F. Lekien, and J.E. Marsden. Definition and properties of Lagrangian coherent structures from finite time Lyapunov exponents in two-dimensional aperiodic flows. *Physica D*, 212:271–304, 2005.

[18] G. Haller and G. Yuan. Lagrangian coherent structures and mixing in two dimensional turbulence. *Physica D*, 147:352–370, 2000.

[19] F. Lekien, C. Coulliette, A. J. Mariano, E. H. Ryan, L. K. Shay, G. Haller, and J.E. Marsden. Pollution release tied to invariant manifolds: A case study for the coast of florida. *Physica D*, 210:1–20, 2005.

[20] M. Manikandan, G. Haller, T. Peacock, J. E. Ruppert-Felsot, and H. L. Swinney. Uncovering the Lagrangian skeleton of turbulence. *Phys Rev Lett*, 98(14):pp 144502, 2007.

[21] M. Krieg and K. Mohseni. Thrust characterization of pulsatile vortex ring generators for locomotion of underwater robots. *IEEE J. Oceanic Engineering*, 33(2):123–132, 2008.

[22] D. Lipinski, B. Cardwell, and K. Mohseni. A lagrangian analysis of a two-dimensional airfoil with vortex shedding. *J. Phys. A*, 41:344011, 2008.

[23] S.C. Shadden, J.O. Dabiri, and J.E. Marsden. Lagrangian analysis of fluid transport in empirical vortex ring flows. *Physics of Fluids*, 18:7105–7120, 2006.

[24] D. Lipinski and K. Mohseni. A numerical investigation of flow structures and fluid transport with applications to feeding for the hydromedusae Aequorea victoria and Sarsia tubulosa. *submitted to J. Exp. Biology*, 2008.

[25] V. Rom-Kedar and S. Wiggins. Transport in two-dimensional maps. *Archive for Rational Mechanics and Analysis*, 109(3):239–298, 1990.

[26] B. Cardwell and K. Mohseni. Vortex shedding over two-dimensional airfoil: Where do the particles come from? *AIAA J.*, 46(3):545–547, 2008.

[27] B. Cardwell and K. Mohseni. A lagrangian view of vortex shedding and reattachment behavior in the wake of a 2d airfoil. AIAA paper 2007-4231, 37th AIAA Fluid Dynamics Conference and Exhibit, Miami, FL, June 25 - 28 2007.

[28] B. Cardwell and K. Mohseni. Vortex shedding over two-dimensional airfoil: Where do the particles come from? AIAA paper 2008-0423, 46th AIAA Aerospace Sciences Meeting and Exhibit, Reno, Nevada, January 7-10 2008.

[29] B.M. Cardwell and K. Mohseni. Lagrangian coherent structures in the wake of an airfoil. AIAA paper 2007-2771, American Institute of Aeronautics and Astronautics, *Infotech at Aerospace*, Rohnert Park, CA, May 7-10 2007.

[30] G. Haller. Lagrangian coherent structures from approximate velocity data. *Phys. Fluids A*, 14:1851–1861, 2002.

[31] F. Lekien, C. Coulliette, and J.E. Marsden. Lagrangian structures in very high-frequency radar data and optimal pollution timing. *7th Exp. Chaos Conf, AIP*, pages 162–168, 2003.

[32] A.B. Olcay and P.S. Krueger. Measurement of ambient fluid entrainment during laminar vortex ring formation. *Experiments in Fluids*, 44(2):235–247, 2008.

[33] E. Franco, D.N. Pekarek, J. Peng, and J.O. Dabiri. Geometry of unsteady fluid transport during fluid-structure interactions. *Journal of Fluid Mechanics*, 589:125–145, 2007.

INSTRUCTIONS FOR COMPLETING SF 298

1. REPORT DATE. Full publication date, including day, month, if available. Must cite at least the year and be Year 2000 compliant, e.g. 30-06-1998; xx-06-1998; xx-xx-1998.

2. REPORT TYPE. State the type of report, such as final, technical, interim, memorandum, master's thesis, progress, quarterly, research, special, group study, etc.

3. DATES COVERED. Indicate the time during which the work was performed and the report was written, e.g., Jun 1997 - Jun 1998; 1-10 Jun 1996; May - Nov 1998; Nov 1998.

4. TITLE. Enter title and subtitle with volume number and part number, if applicable. On classified documents, enter the title classification in parentheses.

5a. CONTRACT NUMBER. Enter all contract numbers as they appear in the report, e.g. F33615-86-C-5169.

5b. GRANT NUMBER. Enter all grant numbers as they appear in the report, e.g. AFOSR-82-1234.

5c. PROGRAM ELEMENT NUMBER. Enter all program element numbers as they appear in the report, e.g. 61101A.

5d. PROJECT NUMBER. Enter all project numbers as they appear in the report, e.g. 1F665702D1257; ILIR.

5e. TASK NUMBER. Enter all task numbers as they appear in the report, e.g. 05; RF0330201; T4112.

5f. WORK UNIT NUMBER. Enter all work unit numbers as they appear in the report, e.g. 001; AFAPL30480105.

6. AUTHOR(S). Enter name(s) of person(s) responsible for writing the report, performing the research, or credited with the content of the report. The form of entry is the last name, first name, middle initial, and additional qualifiers separated by commas, e.g. Smith, Richard, J, Jr.

7. PERFORMING ORGANIZATION NAME(S) AND ADDRESS(ES). Self-explanatory.

8. PERFORMING ORGANIZATION REPORT NUMBER. Enter all unique alphanumeric report numbers assigned by the performing organization, e.g. BRL-1234; AFWL-TR-85-4017-Vol-21-PT-2.

9. SPONSORING/MONITORING AGENCY NAME(S) AND ADDRESS(ES). Enter the name and address of the organization(s) financially responsible for and monitoring the work.

10. SPONSOR/MONITOR'S ACRONYM(S). Enter, if available, e.g. BRL, ARDEC, NADC.

11. SPONSOR/MONITOR'S REPORT NUMBER(S). Enter report number as assigned by the sponsoring/ monitoring agency, if available, e.g. BRL-TR-829; -215.

12. DISTRIBUTION/AVAILABILITY STATEMENT. Use agency-mandated availability statements to indicate the public availability or distribution limitations of the report. If additional limitations/ restrictions or special markings are indicated, follow agency authorization procedures, e.g. RD/FRD, PROPIN, ITAR, etc. Include copyright information.

13. SUPPLEMENTARY NOTES. Enter information not included elsewhere such as: prepared in cooperation with; translation of; report supersedes; old edition number, etc.

14. ABSTRACT. A brief (approximately 200 words) factual summary of the most significant information.

15. SUBJECT TERMS. Key words or phrases identifying major concepts in the report.

16. SECURITY CLASSIFICATION. Enter security classification in accordance with security classification regulations, e.g. U, C, S, etc. If this form contains classified information, stamp classification level on the top and bottom of this page.

17. LIMITATION OF ABSTRACT. This block must be completed to assign a distribution limitation to the abstract. Enter UU (Unclassified Unlimited) or SAR (Same as Report). An entry in this block is necessary if the abstract is to be limited.